3C3-5

Performance of Adaptive Beamforming with Multiport Parasitic Array Radiator Antenna

#Masayuki Morishita [1,2], Chen SUN [2], Makoto Taromaru [2], Hiroyoshi Yamada [1,2], Takashi Ohira [2]

[1] *Graduate School of Science & Technology, Niigata University*
Ikarashi 2-8050, Niigata 950-2181, Japan, {morisita,yamada}@wave.ie.niigata-u.ac.jp

[2] *ATR Wave Engineering Laboratories*
2-2-2 Hikaridai, 'Keihanna Science City', Kyoto, 619-0288, Japan, {sun,taromaru,ohira}@atr.jp

1. Introduction

Modern wireless communications systems require improvement in capacity and data transmission speed. Adaptive array antennas separate spatially a desired wave from interference waves by controlling their radiation or beam pattern directivity. A digital beamforming (DBF) array performs adaptive beamforming by digital signal processing. However, the circuit scale, number of RF channels and power consumption increase with the number of array elements.

In this paper, we propose a system of adaptive beamforming with multiport parasitic array radiator (MuPAR) antenna [1]. We apply the combination of a DBF and an analog beamforming algorithms at the MuPAR. The MuPAR consists of multiple active elements and parasitic elements. The parasitic elements are loaded with variable reactors. Since these elements are placed near the active elements, there is inducing strong electromagnetic coupling between parasitic and active ones. These parasitic elements operate as directors or reflectors by adjusting reactance of variable reactors. Compared with a DBF array having the same number of elements, the MuPAR structure is composed of less RF channels and A/D converters, thus has less power consumption. The goal of this paper is to examine the performance of adaptive beamforming with the MuPAR. We apply the steepest gradient algorithm (SGA) [2] to optimize the reactances; and apply RLS algorithm [3] to perform DBF at the active elements. We compare adaptive beamforming performance with DBF array.

2. Signal Model

The proposed MuPAR antenna consists of N active elements and M parasitic elements. Figure 1 shows an example of the antenna having $N = 2$ active and $M = 2$ parasitic elements considered in this paper. There are d impinging signals $s_k(t)$ with direction of arrivals (DoAs) $(\phi_k)(k = 1, 2, \cdots, d)$. Let us denote $\boldsymbol{a}(\phi_k)$ as the steering vector of the MuPAR. The output signals at the N RF ports of the MuPAR can be written as

$$\boldsymbol{x}(t) = \boldsymbol{i}^T \sum_{k=1}^{d} \boldsymbol{a}(\phi_k) s_k(t) + \boldsymbol{n}(t) \quad (1)$$

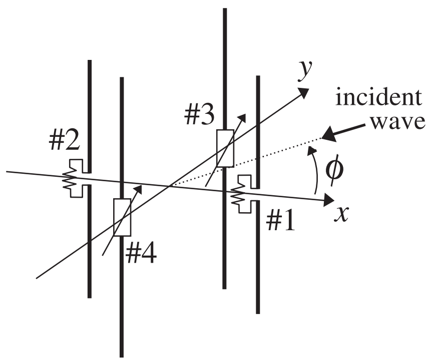

Figure 1 Geometry of MuPAR. $N = 2, M = 2$.

where $\boldsymbol{n}(t)$ is additive white Gaussian noise at the receiver, and ^{T} is the transpose of a vector or matrix. $\boldsymbol{i}$ is the current vector, given by [4] as

$$\boldsymbol{i} = \left(\boldsymbol{Y}^{-1} + \boldsymbol{Z} + \boldsymbol{X}\right)^{-1} \boldsymbol{U} \quad (2)$$

ISBN: 978-4-88552-223-9 C3055©IEICE

where the matrix $\boldsymbol{Z} = diag[z_1, z_2, \cdots, z_N, 0, \cdots, 0]$ is a diagonal matrix which consists of feed impedances, and the matrix $\boldsymbol{X} = diag[0, \cdots, 0, jX_1, jX_2, \cdots, jX_M]$ is a diagonal matrix called the reactance matrix. Moreover, the matrix $\boldsymbol{Y}$ components are mutual admittances between the array elements. Matrix $\boldsymbol{U}$ is defined as

$$\boldsymbol{U} = \begin{bmatrix} 1 & \cdots & 0 & 0 & \cdots & 0 \\ \vdots & \ddots & \vdots & \vdots & \ddots & \vdots \\ 0 & \cdots & 1 & 0 & \cdots & 0 \end{bmatrix}^T \tag{3}$$

3. Adaptive Algorithm

We apply a combination of SGA and RLS algorithm to perform adaptive beamforming with the MuPAR. The flowchart of optimization of the adaptive algorithm is illustrated in Figure 2. The first step is optimization of the reactances by SGA with given weight for the active elements. The second step is optimization of the weights by RLS with the reactances. After optimization is completed, convergence of output SINR is judged. The optimization sequence is repeated until the output SINR is converged. The block diagram of MuPAR is shown in Figure 3.

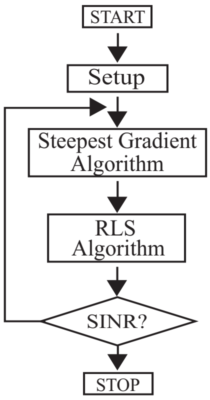

Figure 2 Flowchart of adaptive beamforming with a MuPAR

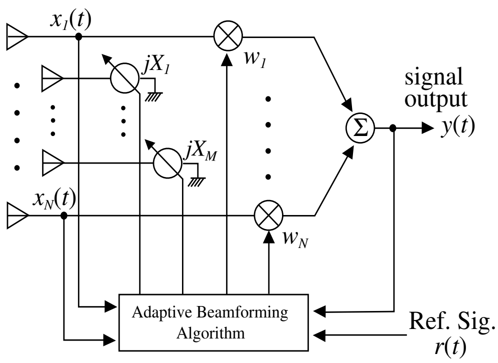

Figure 3 Functional block diagram of MuPAR

3.1 RLS Algorithm

The weight determination algorithm for the MMSE-based RLS algorithm. The algorithm determines knowing the output signals at $N = 2$ active elements in Eq.(1), the output after apply DBF at the two RF ports is given as

$$y(m) = \boldsymbol{w}^H(m)\boldsymbol{x}(m) \tag{4}$$

where m is the iteration index. The optimal weights are iteratively determined by minimizing the error between the reference signal $r(m)$ and the output signal $y(m)$, which is given by [3]

$$|e(m)|^2 = |r(m) - y(m)|^2 = |r(m) - \boldsymbol{w}^H\boldsymbol{x}(m)|^2 \tag{5}$$

$\boldsymbol{x}(m)$ is the received signal and ^{H} is the transpose and conjugate operation. In the RLS algorithm, the weight determination equations of the $(m+1)$th iteration are given by [3]

$$\boldsymbol{w}(m+1) = \boldsymbol{w}(m) + \gamma \boldsymbol{R}_{xx}^{-1}(m)\boldsymbol{x}(m+1)e^*(m-1) \tag{6}$$

$$\gamma = \frac{1}{\alpha + \boldsymbol{x}^H(m+1)\boldsymbol{R}_{xx}^{-1}(m)\boldsymbol{x}(m+1)} \tag{7}$$

where $\boldsymbol{R}_{xx}$ is the correlation matrix of the received signal and α is forgetting factor.

3. 2 Steepest Gradient Algorithm

We briefly describe a SGA of the MuPAR. In this algorithm, a reference signal $r(t)$ is used, which is assumed to be known in receiver. As for the steepest gradient method, the updated value of the reactance vector at the $(m+1)$th iteration is given by

$$\boldsymbol{X}(m+1) = \boldsymbol{X}(m) + \mu \nabla \rho_m \tag{8}$$

where μ is a positive real-value constant which controls the convergence speed. An estimate of the gradient vector $\nabla \rho_m$ of Eq.(8) may be obtained by the use of finite-difference approximations of derivative [5], [6]. In our algorithm a maximum cross correlation coefficient (MCCC) ρ_m is adoped. We assume that $\boldsymbol{y}(m)$ and $\boldsymbol{r}(m)$ are the P-dimensional column vectors that are discrete time samples of $y(t)$ and $r(t)$, respectively. The MCCC between $\boldsymbol{y}(m)$ and $\boldsymbol{r}(m)$ at the m-th iteration is define by [2]

$$\rho_m = \frac{|\boldsymbol{y}^H(m)\boldsymbol{r}(m)|}{\sqrt{\boldsymbol{y}^H(m)\boldsymbol{y}(m)}\sqrt{\boldsymbol{r}^H(m)\boldsymbol{r}(m)}} \tag{9}$$

It is well known that the MCCC represents the similarity of two signals, while the error represents the difference. Note that the correlation coefficient of Eq.(9) is normalized. The interference component in the output signal $y(t)$ is suppressed when $y(t)$ becomes "similar" to the reference signal $r(t)$ regardless of their difference in amplitude.

4. Simulation

In this section, we show performance of the adaptive beamforming with MuPAR that combines the optimization algorithms shown in Section 3. The MuPAR considered has two active elements $N = 2$ (#1, #2) and two parasitic elements $M = 2$ (#3, #4) as shown in Figure 1. The inter-element spacing is $\lambda/4$, and the elements are dipole antennas of half-wavelength. The MCCC defined in Eq.(9) is calculated with $P = 10$; and the value of the step-size parameter μ in Eq.(8) is assigned to 150. Number of iterations of RLS and SGA is 20 and 30 times, respectively. The adaptive beamforming of MuPAR, which combives RLS and SGA optimization stages, is repeated 10 times. Therefore, the total number of the iteration is $(20 + 30) \times 10 = 500$.

Let's first consider the case where there are three signals coming from different directions. The SNR is 20 dB and the input SIR is 0 dB, assuming the equal powers of the signals. The desired signal and the interference signals are incoherent. The initial value of each reactance is set to zero. Figure 4(a) shows the convergence curve over 500 iterations. The formed beam pattern after iteration is shown in figure 4(b). The beam is steered to the desired signal at 100°, while the deep nulls are formed towards the interference signals at 45° and 285°.

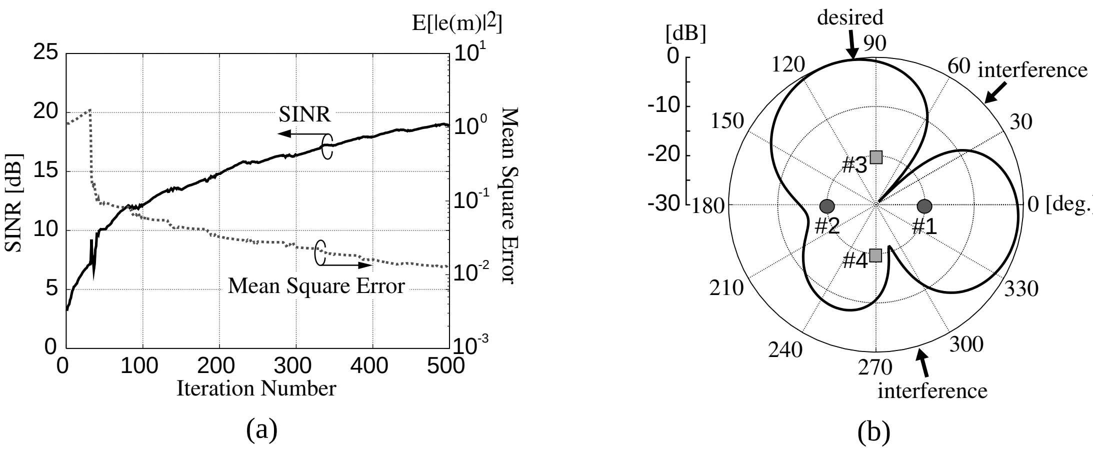

Figure 4 (a) Convergence property of SINR. (b)Antenna pattern after 500 iteration. DoAs are [100°,45°,285°] and DOA of desired is 100°.

Second, we consider the statistical performance of the output SINR of the adaptive beamforming with MuPAR. We compare its performance with 2,3, and 4-element DBFs. The geometry of the 2-element DBF is same as the active elements of MuPAR. The 3-element DBF is trigonal array equally spaced between the array elements. The 4-element DBF has the same element layout as MuPAR. DOA of the desired signal is fixed at 90°, and the DOA(s) and those of the two interference signals are randomly generated according to a uniform distribution over $[0°, 359°]$. Ten thousand totals are used to calculate the empirical complementary cumulative distribution function (CCDF) of the output SINR. The performance of the adaptive beamforming with MuPAR is significantly much better than the DBF of 2-element array. The performance of the MuPAR adaptive beamforming is equivalent to that of the 3-element DBF.

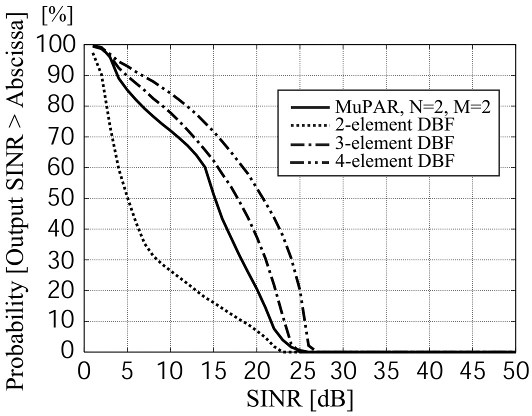

Figure 5 Output SINR of the abscissa after iteration of 500.

5. Conclusions

In this paper, we evaluated a MuPAR antenna performance, and applied the combination of DBF and analog beamforming. We applied the SGA to optimize the reactances and applied RLS algorithm at active elements. The algorithm makes the MuPAR steer its beam and nulls automatically. After the system model was given the performance of the proposed scheme was examined. The MuPAR can be adaptive beamforming at three incident waves. The structure of the MuPAR enables adaptive beamforming to be improved with less power consumption circuit scale. Adaptive beamforming of MuPAR is equivalent to 3-element DBF. Much better performance than the 2-element DBF is achieved with a MuPAR which has only two additional parasitic elements. The structure features low power consumption and fabrication cost. Thus, the proposed adaptive beamforming with MuPAR is a suitable for implementing adaptive antennas for mobile terminals.

References

[1] M. Ohira, A. Miura, M. Ueba, M. Taromaru, T, Ohira, ”Varactor–Loaded Inverted–F Multiport Parasitic Array Radiator Antenna,” IEEE AP–S Symp, July 2007. (Submitted)

[2] J. Cheng, Y. Kamiya, and T. Ohira, ”Adaptive beamforming of ESPAR antenna based on steepest gradient algorithm,” IEICE Trans. Commun., vol.E 84–B, no.7, pp.1790–1800. July 2001.

[3] N. Kikuma, Adaptive signal processing with Array Antenna, Science and Technology Publishing Company, Tokyo, 1999

[4] T. Ohira, K. Iigusa, ”Electronically steerable parasaitic array radiator antenna,” IEICE, Trans. Electronics Vol.J87–C, no.1 pp.12–31, Jan. 2004.

[5] R.A. Monzingo and T.W. Miller, Introduction to Adaptive Arrays, John Wiley & Sons, Inc., 1980.

[6] J. Van de Degte, Feedback Control System, Third Edition, Prentice Hall, 1994.